

Selectively Permeable Dendrimers as Molecular Gates

by Gregory P. Perez and Richard M. Crooks

Polymeric materials are commonly used to control mass transfer between liquid phases and surfaces to prevent corrosion or to selectively pass ions in energy producing devices and chemical sensors. Polymers are also useful for enabling gas separations. Applications such as these are of tremendous importance to industry, and even modest improvements in performance can yield dramatic effects on the economic competitiveness of businesses and nations. It is not surprising, therefore, that scientists and engineers in academics, government laboratories, and industry dedicate substantial resources to the development of new polymeric materials that offer enhancements for small molecule discrimination.

This short article is about dendrimers and how they can be used to prepare exquisitely selective nanoscopic chemical filters. Dendrimers, which were first reported by Vögtle in 1978,¹ are nearly monodisperse (and sometimes truly monodisperse) polymers with well-defined geometrical and chemical structures (Fig. 1). Because of their uniform properties dendrimers, and related materials such as hyperbranched polymers,² they provide a valuable model for correlating macromolecular structure to technological function.

Dendrimers are prepared by either a convergent³ or divergent⁴ approach, and the interested reader is referred to excellent recent reviews to learn more about the vast range of dendritic materials that have been prepared by these two methods.⁵⁻⁷ For illustrative purposes, we shall limit the discussion here to the commercially available poly(amidoamine) (PAMAM) family of dendrimers. PAMAM dendrimers are prepared by the divergent approach, which means they are synthesized outwards from a central core, often ethylene diamine, by an iterative series of two reactions: Michael addition followed by amidation. The first iteration of these two reactions results in a zero generation (G0) PAMAM dendrimer. Subsequent iterations result in higher generation materials. The chemical structure of a G2 PAMAM dendrimer is

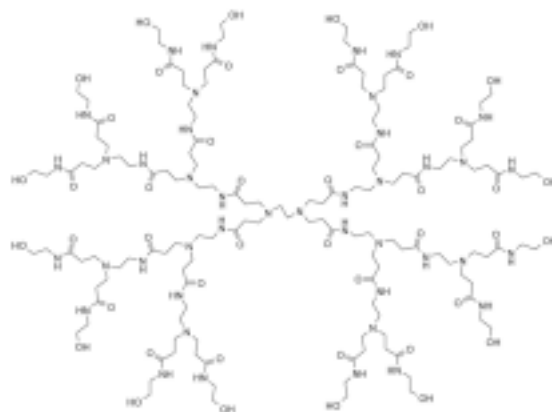


Fig. 1. Structure of a second-generation, hydroxyl-terminated PAMAM dendrimer (G2OH).

shown in Fig. 1. (Note that in this case the last amidation reaction was performed with ethanolamine to leave the dendrimer terminated with hydroxyl groups.) Dendrimers have three properties that make them unique among macromolecules. First, the extent of steric crowding on the dendrimer periphery can be controlled. Second, there is a somewhat hollow region within the interior of high molecular weight dendrimers. Third, the large number of functional groups on the dendrimer surface can be varied to impart interesting chemical properties.

PAMAM dendrimers range in diameter from about 2 nm (G1) up to about 13 nm (G10). The molecular weight and number of peripheral groups of dendrimers increase exponentially with each generation, while the diameter increases more or less linearly. These facts account for the interesting physical structure of dendrimers. That is, with each ensuing generation the surface density of peripheral moieties, most commonly primary amines or hydroxyl groups, increases. The conformation of dendrimers adjusts to this steric crowding by developing a three-dimensional structure. For example, a G1 or G2 PAMAM dendrimer has an open, flat structure, but by G4 the 64 peripheral

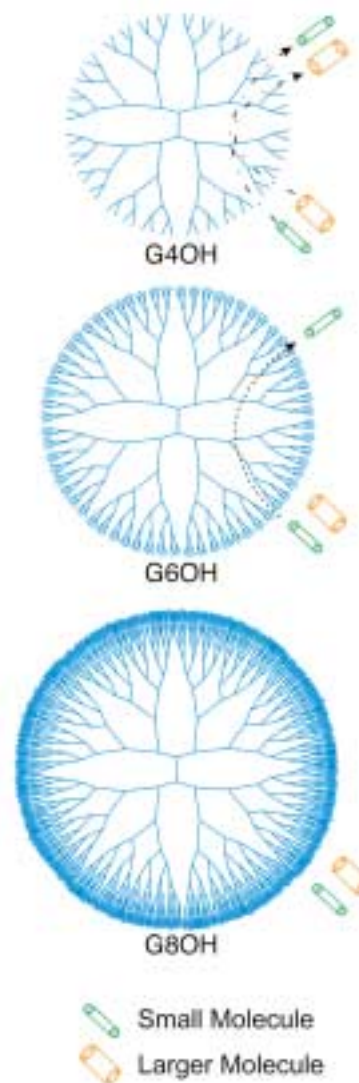


Fig. 2. Schematic illustration of the principle of size-selective permeability as a function of dendrimer generation. Steric crowding on the dendrimer periphery increases as a function of generation, thereby reducing permeability. Reproduced with permission from J. Am. Chem. Soc. Copyright 2001 Am. Chem. Soc.

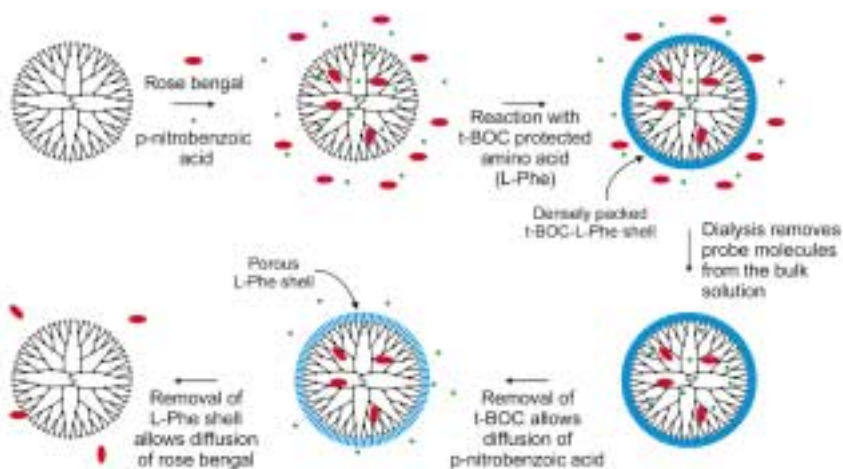


FIG. 3. Schematic representation of Meijer's "dendritic box" experiment. The experiment is described in the text.

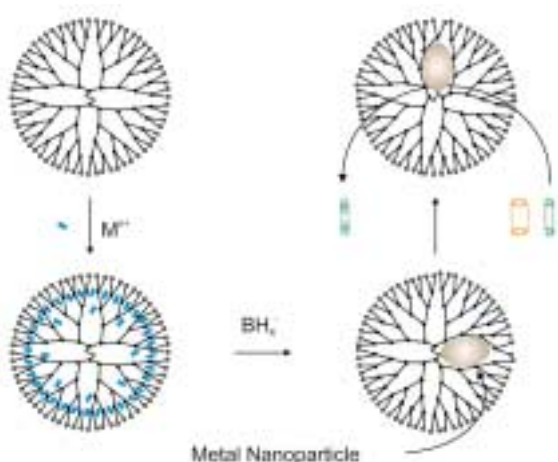


FIG. 4. Preparation of dendrimer-encapsulated catalysts (DECs). Metal ions in solution, such as copper, gold, platinum, or palladium, partition into the dendrimer interior. Addition of a reducing agent, such as BH_4^- , results in formation of a dendrimer-encapsulated metal nanoparticle replica within the dendrimer template. Access of substrates to the nanoparticle is mediated by chemical and physical properties of the dendrimer.

groups can only be accommodated if the 4.5 nm-diameter dendrimer becomes spheroidal. By G8 the number of terminal groups has increased to 1024, but the diameter (compared to G4) has only doubled, and therefore the periphery is very densely packed. The surface density of functional groups increases from about $1.0/\text{nm}^2$ for G4 to $3.5/\text{nm}^2$ for G8, which of course means that the average spacing between dendrimer terminal groups is reduced as the generation increases. It seemed reasonable to us that it would be possible to take advantage of this property to control small-molecule permeation through dendrimers. That is, as shown in Fig. 2, almost any relatively small molecule should be able to penetrate the open periphery of the G4 PAMAM dendrimer, while such molecules would have a far more difficult time moving through the close-packed G8 periphery. In addition to this sort of size/shape physical control over dendrimer permeability, the rich chemistry of the dendrimer periphery can also be used to control through-dendrimer mass transport.

The Dendritic Box

Many of the essential concepts underlying the use of dendrimers as selective filters are embodied in Meijer's "Dendritic Box".^{8,9} This is a 'trap-and-release' experiment, which takes advantage of all three dendrimer properties mentioned earlier: the hollow interior, the high density of functional groups on the exterior, and the chemical flexibility of the periphery. Meijer used poly(propyleneimine) (PPI) dendrimers, which are very closely related to the PAMAM family, as the scaffolds for this experiment. Figure 3 illustrates his general approach. First, a high generation PPI dendrimer was mixed with a solution containing the dye rose bengal (RB) and a smaller dye, *p*-nitrobenzoic acid (*p*NBA). As with any dynamic equilibrium, both dye molecules are able to enter and exit the dendrimeric structure. At equilibrium a significant fraction of both molecules partition into the hollow dendrimer interior. Next, the terminal dendrimer amine groups are reacted with a *t*BOC-protected phenylalanine amino acid (N-*t*BOC-L-

Phe). These bulky moieties increase steric crowding of the dendrimer periphery sufficiently that RB and *p*NBA present within the dendrimer interior at the moment of reaction are trapped. Purification by dialysis removes dye molecules from the bulk solution but not from the interior of the 64-Phe-box dendrimers, which are retained within the dialysis sack. Hydrolytic cleavage of the *t*BOC portion of the terminal groups with acid perforates the dendritic box, and the small *p*NBA molecules are once again able to come into equilibrium with the bulk solution. However, this cleavage reaction leaves behind L-Phe at the dendrimer surface, which is itself sufficiently bulky to retain the larger rose bengal molecules. Subsequent hydrolysis of L-Phe results in the original amine-terminated PPI dendrimer and release of RB. This very clever experiment shows how dendrimers can be used to modulate intradendrimer mass transfer.

Dendrimer-Encapsulated Nanoparticles

We recently reported a strategy for encapsulating metal and semiconductor nanoparticles within dendrimers using an approach that is somewhat related to the dendritic box described above.^{10,11} Our approach is shown in Fig. 4. First, a solution of metal ions, such as copper, gold, platinum, or palladium, is mixed with an aqueous PAMAM dendrimer solution. Because PAMAM dendrimers contain tertiary amines within their interior, and because tertiary amines are good ligands for many transition metal ions, the metal ions in solution partition into the dendrimer interior. In many cases the metal ions are held within the interior nearly irreversibly. Addition of a reducing agent, such as BH_4^- , results in conversion of the encapsulated ions to neutral atoms which quickly coalesce into a single metal nanoparticle.

One can think of this approach as a template synthesis in which the dendrimer is the template and the nanoparticle the replica. It is also productive to think of this as a "ship-in-a-bottle" synthesis, because the small metal ions are first introduced into the dendrimer, and then they are assembled into a larger structure (the nanoparticle), which is sterically confined to the dendrimer interior. As we will see in the next section, access of small molecules to the metal particle within the dendrimer can be modulated by controlling the extent of steric crowding on the dendrimer periphery.

Selective Homogeneous Catalysis

We recently developed an approach for using dendrimers as size-selective nanoscopic filters to control mass transport of small molecules within dendrimers. In this section we describe an illustrative example in which an intrinsically nonselective catalyst is rendered selective by addition of a dendritic “nanofilter.” To demonstrate this function we chose to examine the catalytic hydrogenation of alkenes using dendrimer-encapsulated catalysts (DECs) consisting of Pd nanoparticles within high-generation PAMAM dendrimers.^{12,13} As shown in the final frame of Fig. 4, the idea is that only substrate molecules small enough to penetrate the dendrimer periphery are able to move into the interior, encounter the catalyst, and react with H₂ to yield the corresponding alkane. The rate of substrate penetration directly correlates to the amount of alkane present in solution, which can be measured by NMR spectroscopy.

To demonstrate the function of a size-selective dendritic nanofilter we used a series of three DECs based on hydroxyl-terminated PAMAM dendrimers of generation 4, 6, and 8 (G4OH, G6OH, and G8OH). Each dendrimer contained a Pd nanocluster consisting of, on average, 40 atoms (e.g. G4OH/Pd(0)40). These DECs were challenged with allyl alcohol and four allylic alcohol derivatives substituted at the α position with the following groups: methyl, ethyl, dimethyl, and methyl-ethyl.¹³ The experiment was carried out by exposing each of the three DECs to each of the five alcohols and then measuring the turnover frequency (TOF, mol of H₂ per mole of Pd(0) per hour) of the alkene groups.

The results of this study (Table I) indicate that as the substrate size increases for a particular generation of dendrimer, the hydrogenation TOF decreases. Similarly, for a particular substrate, the TOF decreases as the dendrimer size increases. For example, the maximum TOF for the G4OH/Pd(0)40 catalyst for the hydrogenation of allyl alcohol (1) was 475 ± 5 mol H₂(mol Pd)⁻¹ h⁻¹. A substrate having one α methyl group (2) yielded a slightly lower TOF. When the methyl group was changed to ethyl (3), the reaction rate decreased further to 260 mol H₂(mol Pd)⁻¹ h⁻¹. This trend continues when two methyl groups are present at the α position (4) and when both a methyl and an ethyl group are present at the α position of

Table I. Hydrogenation reaction rates using GnOH/Pd(0)40 catalysts for structurally related allylic alcohols.

Substrates	TOF[mol H ₂ (mol Pd) ⁻¹ h ⁻¹]		
	G4OH/Pd(0) 40	G6OH/Pd (0) 40	G8OH/Pd (0) 40
(1) 	480/470 ¹	450/460 ¹	120
(2) 	450/460 ¹	380	93
(3) 	260	280	68
(4) 	150	75	62
(5) 	100	40	50

Hydrogenation reactions were carried out at $25 \pm 2^\circ\text{C}$ with 2×10^{-4} M Pd(0) composite catalysts in MeOH-H₂O (4:1 v/v) mixtures. The turnover frequency (TOF) was calculated based on H₂ uptake (mol of H₂ per mol of Pd(0) per hour).

¹ Duplicate measurements were performed to illustrate the level of run-to-run reproducibility.

the substrate (5). Overall, the TOF for the bulkiest substrate (5) was nearly five times lower than the smallest (1). The same trend is apparent for the G6OH/Pd(0)40 and G8OH/Pd(0)40 DECs. It is also interesting to compare hydrogenation rates for a particular substrate when different generation dendrimers encapsulate the Pd(0) nanoparticle. Table I shows that there is a clear trend in this regard too: lower generation DECs, with just two exceptions, result in the highest TOFs.

These findings can be rationalized in terms of the “mesh” size of the dendrimers, which can be estimated using molecular modeling. Specifically, if a few reasonable assumptions are made,¹³ the average spacing between adjacent van der Waals surfaces of the hydroxyl groups of G4OH, G6OH, and G8OH turns out to be 8.2, 5.4, and 3.2 Å, respectively. These values can be compared to the substrate sizes, which we have correlated to the largest linear dimension perpendicular to the O-H bond direction. These values are: 5.5, 7.0, 7.5, 7.0, and 8.0 Å for substrates 1-5, respectively. The close correlation between these values and the data in Table I suggest that the simple size-exclusion model embodied by Fig. 2 is a good first approximation. However, there is enough variation in this static model to suggest that both time-dependent motion of the dendrimer and chemical interactions between the dendrimer and substrate also contribute to the selectivity of DECs. The latter issue is explored in the next sections.

Surface-Confined Dendrimers

Up to this point we have only discussed homogeneous solutions where the dendrimer periphery was utilized to mediate access to the interior. However, it is also possible to immobilize dendrimers on solid surfaces, and we have shown that even when surface-confined, the dendrimer periphery can be used to mediate intradendrimer mass transport and thereby impart selectivity to the surface.

PAMAM dendrimers form stable, densely packed monolayers via polydentate interactions with Au and other substrate materials.¹⁴ It is also possible to prepare mixed monolayers on Au consisting of dendrimers and *n*-alkanethiols, which provides a means for studying isolated dendrimers on surfaces. Chemically more robust dendrimer monolayers can be prepared by covalently linking the dendrimer to an intermediate molecular adhesion promoter.^{15,16} These approaches can be used to control access of small molecules to both the dendrimer interior and the underlying surface.

Dendrimer-Induced Gating at the Solid-Liquid Interface

It is possible to control access of small molecules to a surface using mixed monolayers consisting of dendrimers and *n*-alkanethiols, and the selectivity imparted to the surface can arise from either physical or chemical interactions between the substrate and the dendrimer.¹⁷ That is, mixed monolayers yield dendrimeric gates separated from one

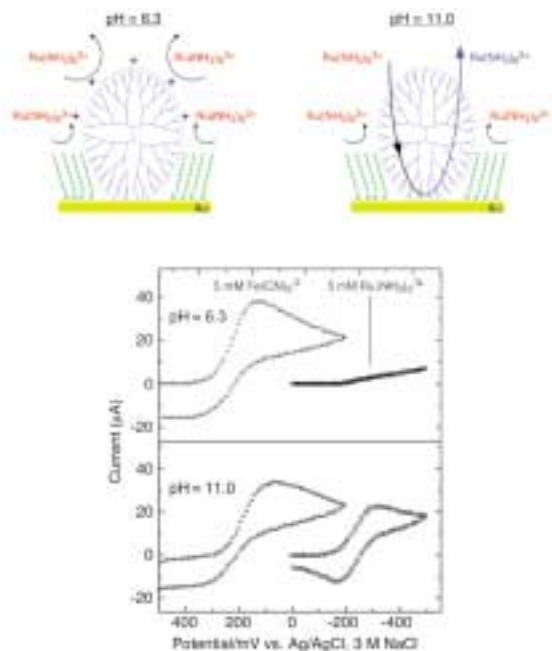


Fig. 5. (Top) Dendrimers within n-alkanethiol SAMs act as single-molecule gates. The SAM serves to passivate the underlying Au electrode and the dendrimer selectively passes ions depending on the chemical state of the dendrimer and the charge on the ion. (Bottom) Cyclic voltammetry of 5 mM $\text{Fe}(\text{CN})_6^{3-}$ and 5 mM $\text{Ru}(\text{NH}_3)_6^{3+}$ in 0.5 M aqueous Na_2SO_4 electrolyte solutions at $\text{G4NH}_2/\text{C16SH}$ -modified Au electrodes: (a) pH = 6.3 (0.025 M Na_2HPO_4 + 0.025 M NaH_2PO_4), and (b) pH = 11 (0.036 M NH_4Cl + 2.0 M NH_4OH). Electrode area: $0.09 \pm 0.009 \text{ cm}^2$, scan rate: 50 mV/s.

another by fully passivated regions of n-alkanethiol as shown at the top of Fig. 5.

The bottom of Fig. 5 shows cyclic voltammetric data obtained from a mixed monolayer consisting of amine-terminated G4 PAMAM dendrimers (G4NH_2) and hexadecane thiol (C16SH). At pH = 6.3 the amine terminal groups of the dendrimers are protonated (pK_a about 9.5) and effectively block penetration of bulk-phase $\text{Ru}(\text{NH}_3)_6^{3+}$, which is used as a mass transport reporter probe, and therefore no Faradaic current is observed. In contrast, the rate of reduction of negatively charged $\text{Fe}(\text{CN})_6^{3-}$ is only slightly hindered compared to a naked Au electrode. Contrast these results with those obtained at pH = 11.0 when the primary amine groups are in their neutral form. In this case both $\text{Fe}(\text{CN})_6^{3-}$ and $\text{Ru}(\text{NH}_3)_6^{3+}$ penetrate the dendrimer portion of the mixed SAM. This result alone, however, does not definitively prove pH-regulated intradendrimer mass transport of the redox probes, because the observed effects could arise from probe penetration at the interface between G4NH_2 and C16SH. Because of the strong compressive force exerted on the dendrimers by C16SH, we thought this was an unlikely scenario, but to prove that the dendrimers themselves, rather than dendrimer-induced defects in the monolayer, are acting as molecular gates we performed the additional experiments discussed next.

A mixed monolayer consisting of G4NH_2 and C16SH was prepared as

described earlier, but in this case we converted the terminal amines to 4-(trifluoromethyl)benzamido groups. Next we compared the voltammetry of $\text{Fe}(\text{CN})_6^{3-}$ at pH 6.3 at this modified electrode surface to the $\text{G4NH}_2/\text{C16SH}$ monolayer (Fig. 5). The results indicated that while the protonated amine periphery of G4NH_2 passes $\text{Fe}(\text{CN})_6^{3-}$ (Fig. 5), the bulky and hydrophobic 4-(trifluoromethyl)benzamido groups prevent penetration. If penetration occurred at defects at the $\text{G4}/\text{C16SH}$ interface rather than through the dendrimer interior, then we might anticipate identical responses for the fluorinated and unfluorinated dendrimers.

A second experiment provides additional evidence for intradendrimer mass transfer of the redox probes. In this case electrodes were modified with mixed monolayers composed of either G0, G4, or G8 dendrimers and C16SH, and then the voltammetry was examined at pH = 6.3. The important result is that for both $\text{Ru}(\text{NH}_3)_6^{3+}$ and $\text{Fe}(\text{CN})_6^{3-}$ the Faradaic current decreased as a function of increasing dendrimer generation. As for the homogeneous catalysis results described earlier, this result is a consequence of increased steric crowding on the dendrimer periphery as the generation increases. This in turn leads to a corresponding reduction in probe penetrability.

There are three important conclusions that arise from this set of experiments. First, surface-confined dendrimers only 3

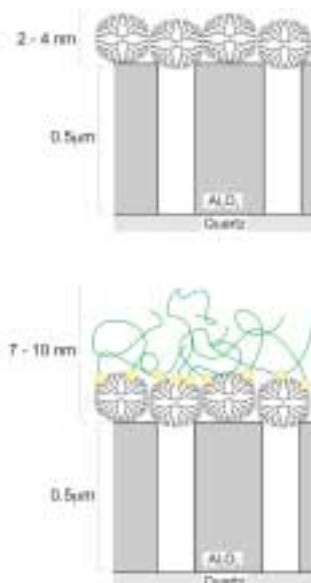


Fig. 6. Schematic illustration of a method for using dendrimers to selectively filter vapor-phase molecules. The substrate is a nanoporous alumina thin film confined to the active region of a surface acoustic wave (SAW) nanogravimetric mass balance. (Top) a dendrimer monolayer films. (Bottom) a composite dendrimer/Gantrez coating prepared by sequential reaction.

nm in thickness are able to quantitatively control access of small molecules to an underlying solid substrate. Second, trans-dendrimer mass transport can be controlled by primarily physical means (steric crowding on the dendrimer periphery realized by either increasing the dendrimer generation or by addition of bulky groups to relatively low generation dendrimers) or by chemical means (electrostatic repulsion). Third, and perhaps most important for future applications, it is possible to exert active control over intradendrimer mass transport (in this case by modulating the pH).

Vapor-Phase Gating Using Dendrimers

The previously described results addressed intradendrimer mass transport in liquid phases. This final section briefly discusses some very preliminary results from experiments presently underway in our lab that are focused on intradendrimer mass transport in vapor phases. These new studies build upon previous results from our group, which showed that dendrimers could be used as molecular recognition elements for vapor-phase sensing applications.¹⁸ Now, rather than using dendrimers to simply trap volatile organic compounds (VOCs), we are trying to develop a means for filtering them through individual dendrimers. Our approach is shown in Fig. 6.

We began these studies by immobilizing dendrimers atop alumina substrates,

provided to us by Graham Yelton and his colleagues at Sandia National Laboratories, that contain pores having relatively monodisperse, nanometer-scale diameters.¹⁹ Because dendrimer diameters (~1-13 nm) are fairly well matched in size with the pore diameter of the substrate, which can be as small as 2 nm, we envisioned that it might be possible to immobilize a single dendrimer above each pore. The idea is that access to the underlying pore would only be allowed if the analyte could enter and exit the dendrimer. By controlling the properties of the dendrimer as we have in the solution-phase studies, we thought it would be possible to control selectivity. Mass transport across the dendrimer can be measured by gravimetry using mass-sensitive surface acoustic wave (SAW) devices.²⁰ Unfortunately, the heterogeneity in the pore size of the alumina substrates has thus far prevented us from satisfactorily demonstrating this approach. The problem is that there are leaks between the dendrimers and pores in the alumina that are larger than the dendrimers.

We are still working to solve the leaking problem by improving the monodispersity of the substrate pores, but in the meantime we have had a fair measure of success by simply plugging the leaks. Specifically, we have shown that a very thin (7-10 nm) composite film consisting of both dendrimers and Gantrez,²¹⁻²³ an active anhydride copolymer, can be used to seal the dendrimer/alumina interface and thereby force VOCs through the dendrimers (bottom of Fig. 6). The results of these studies will be reported shortly.²⁴

Prospects for the Future

In this paper we have shown that dendrimers can be used as nanoscopic molecular filters to selectively control the mass transport of small molecules. This function is introduced by exerting synthetic control over the physical and chemical properties of the dendrimer periphery. For example, high generation dendrimers selectively exclude some allylic alcohol derivatives but pass others. This property was used to convert an intrinsically nonselective catalyst (Pd) into one that is selective. At present we are testing more complex dendrimers that we hope will lead to an even higher level of selectivity.

We have also demonstrated active control over intradendrimer mass transport by modulating the surface charge on pH-sensitive dendrimer terminal groups. This proof-of-concept experi-

ment opens the door to more sophisticated "smart materials" that could modulate access to the dendrimer interior as a function of temperature or the presence of specific chemicals that might be present. Such an approach would be attractive for controlling the rate of reactions that rely on access to dendrimer-encapsulated catalysts.

Finally, we should mention that dendrimers are not likely to find their way into high-volume applications any time soon because of their prohibitive cost. Thus, the commercial value of the results presented here reside mainly in the concepts described and the extent to which they can be introduced into other, less costly, polymers and related materials. However, some applications, such as those involving chemical sensing and bench-scale chemical reactions, require very small quantities of dendrimers, and thus these may represent a direct market trajectory for dendrimeric nanofilters if sufficient value is added by clever scientists and engineers. ■

Acknowledgments

We acknowledge our coworkers past and present who have contributed to the results described in this article: Richard W. Cernosek, Yanhui Niu, Hideo Tokuhisa, W. Graham Yelton, Lee K. Yeung, and Mingqi Zhao. This work was supported by the Office of Naval Research. Additional support was provided via subcontract from Sandia National Laboratories, which is supported by the U.S. Department of Energy (Contract DE-AC04-94AL8500). Sandia is a multiprogram laboratory operated by the Sandia Corporation, a Lockheed-Martin company, for the U.S. Department of Energy.

References

1. E. Buhleier, W. Wehner, and F. Vögtle, *Synthesis*, 155 (1978).
2. B. Voit, *J. Polym. Sci. A*, **38**, 2505 (2000).
3. C. J. Hawker and J. M. Fréchet, *J. Am. Chem. Soc.*, **112**, 7638 (1990).
4. D. A. Tomalia, H. Baker, J. Dewald, M. Hall, G. Kallos, S. Martin, J. Roeck, J. Ryder, and P. Smith, *Polym. J.*, **17**, 117 (1985).
5. A. W. Bosman, H. M. Janssen, and E. W. Meijer, *Chem. Rev.*, **99**, 1665 (1999).
6. O. A. Matthews, A. N. Shipway, and J. F. Stoddart, *Prog. Polym. Sci.*, **23**, 1 (1998).
7. F. Vögtle, S. Gestermann, R. Hesse, H. Schwierz, and B. Windisch, *Prog. Polym. Sci.*, **25**, 987 (2000).
8. J. F. G. A. Jansen, E. M. M. de Brabander-van den Berg, and E. W. Meijer, *Science*, **266**, 1226 (1994).
9. J. F. G. A. Jansen and E. W. Meijer, *J. Am. Chem. Soc.*, **117**, 4417 (1995).
10. M. Zhao, L. Sun, and R. M. Crooks, *J. Am. Chem. Soc.*, **120**, 4877 (1998).

11. R. M. Crooks, M. Zhao, L. Sun, V. Chechik, and L. K. Yeung, *Acc. Chem. Res.*, **34**, 181 (2001).
12. M. Zhao and R. M. Crooks, *Angew. Chem. Int. Ed. Engl.*, **38**, 364 (1999).
13. Y. Niu and R. M. Crooks, *J. Am. Chem. Soc.*, in press.
14. H. Tokuhisa, M. Zhao, L. A. Baker, V. T. Phan, D. L. Dermody, M. E. Garcia, R. F. Peez, R. M. Crooks, and T. M. Mayer, *J. Am. Chem. Soc.*, **120**, 4492 (1998).
15. M. Wells and R. M. Crooks, *J. Am. Chem. Soc.*, **118**, 3988 (1996).
16. H. Tokuhisa and R. M. Crooks, *Langmuir*, **13**, 5608 (1997).
17. M. Zhao, H. Tokuhisa, and R. M. Crooks, *Angew. Chem. Int. Ed. Engl.*, **36**, 2595 (1997).
18. R. M. Crooks and A. J. Ricco, *Acc. Chem. Res.*, **31**, 219 (1998).
19. W. G. Yelton, K. B. Pfeifer, and A. W. Stanton, *J. Electrochem. Soc.*, Submitted.
20. A. J. Ricco, R. M. Crooks, and G. C. Osbourn, *Acc. Chem. Res.*, **31**, 289 (1998).
21. Y. Liu, M. L. Bruening, D. E. Bergbreiter, and R. M. Crooks, *Angew. Chem. Int. Ed. Engl.*, **36**, 2114 (1997).
22. Y. Liu, M. Zhao, D. E. Bergbreiter, and R. M. Crooks, *J. Am. Chem. Soc.*, **119**, 8720 (1997).
23. M. Zhao, Y. Liu, R. M. Crooks, and D. E. Bergbreiter, *J. Am. Chem. Soc.*, **121**, 923 (1999).
24. G. P. Perez, R. M. Crooks, W. G. Yelton, and R. W. Cernosek, In preparation.

About the Authors

Gregory P. Perez received his BS degree in chemistry at Texas A&M University in 1994 and his MS at Southwest Texas State University in 1998. He is presently a doctoral student at Texas A&M University. His research focuses on the synthesis and characterization of new materials for vapor-phase chemical sensors. He can be reached by email at: perez@tamu.edu.

Richard M. Crooks received his Bachelor of Science degree in chemistry from the University of Illinois (Urbana, IL) and his doctoral degree in electrochemistry from the University of Texas (Austin, TX) in 1987. He is currently Professor of Chemistry and Director of the Center for Integrated Microchemical Systems at Texas A&M University (College Station, TX). His research interests include chemical and biological sensors, interfacial design, physical electrochemistry, microfluidics, and catalysis. He can be reached by e-mail at: crooks@tamu.edu.